On Building Communication Maps in Subterranean Environments

Martin Zoula[0000−0002−3235−8176], Miloš Prágr[0000−0002−8213−893X]*, and Jan Faigl[0000−0002−6193−0792]

Faculty of Electrical Engineering, Czech Technical University in Prague,
Technická 2, 166 27, Prague, Czech Republic
{zoulamar,pragrmi1,faiglj}@fel.cvut.cz
https://comrob.fel.cvut.cz

Abstract. Communication is of crucial importance for coordinating a team of mobile robotic units. In environments such as underground tunnels, the propagation of wireless signals is affected by nontrivial physical phenomena. Hence, both modeling of the communication properties and the consequent task to estimate where communication is available becomes demanding. A communication map is a tool assessing the characteristic of communication between two arbitrary spatial coordinates. The existing approaches based on interpolation of a priori obtained spatial measurements do not provide precise extrapolation estimates for unvisited locations. Therefore, we propose to address the extrapolation of the signal strength by a position-independent model based on approximating the obstacle occupancy ratio between the signal source and receiver. The proposed approach is compared to the existing attenuation models based on free-space path loss and spatial projection using a natural cave dataset. Based on the reported results, the proposed approach provides more accurate predictions than the existing approaches.

Keywords: subterranean, communication map, Gaussian process

1 Introduction

In multi-robot scenarios, reliable wireless communication between individual units is an important feature, together with estimating the communication availability in cases where signal propagation is difficult due to natural or artificial constraints. Our research is motivated by deployments of a multi-robot team in communication denied subterranean environments such as cave systems, where most of the signal obstructing mass is static. These environments suffer from nontrivial signal propagation, which cannot be efficiently predicted using simple attenuation models. Even though robots can collaborate without mutual communication while using preset task division algorithms, on-line negotiation is the key factor when reacting to dynamic events. Hence, it is desirable to reliably predict whether and how well a communication channel can be established given the current mission state. A signal propagation model could support tasks like

building communication infrastructure using communication beacons [19]. Also, fast and robust network repairs [4] and reconnection [16] can be maintained. Furthermore, it is possible to predict changes in the network topology [20].

Communication models simulate and approximate the complicated phenomena behind the physical media. The communication models range from statistical Bernoulli or Gilbert-Elliot [7] models to complex raytracing-based physics simulators [22]. The former class yields limited information about modeled communication such as packet delivery probability, yet they are computationally efficient. The latter class tends to involve computationally demanding operations, but yields precise and relevant results, e.g., about the total received power since it accounts for various rigorously defined physical phenomena. Probably the simplest case of physics-based communication models is the *Free-Space Path Loss* (FSPL) attenuation model based on the Friis formula [25]. Note, these approaches rely on a priori known parameters such as signal wavelength or material properties. Besides, setups using no communication model can be used [1], where the robot in need of communication tries to establish a link with another robot by a costly blind broadcast.

Given a communication model that encapsulates the underlying physical media characteristics into a prediction, a communication map is defined as a computational tool determining communication characteristics based on two arbitrary spatial coordinates of the transmitting device and the receiving device. The predicted characteristics may be various, e.g., *Received Signal Strength Indicator* (RSSI) or packet loss ratio. The communication map can be used by a robot to assess the supposed difficulty of communicating to an arbitrary location in the environment. The map can be implemented in various ways, e.g., utilizing self-organizing maps in an acoustic setup as proposed in [6]. However, recent work on communication maps is based on a Gaussian Process (GP) regressor, a soft model that relies on training samples to serve as an interpolation corpus [3,18,2]. Due to the nature of GPs, the model also yields a predictive variance together with the estimate. However, the existing spatial projection method [3] is limited to interpolating the measured data and does not provide satisfiable measurement extrapolations for the unvisited areas.

In this paper, we propose a more general approach to implementing communication maps based on a new computational layer allowing the model to comprehend basic structural properties of the environment. The key benefit of the proposed approach is the ability to extrapolate previous measurements to the so-far unvisited locations. Furthermore, the learned model for one specific environment could be utilized for different environments with similar physical properties. The proposed idea is based on a descriptor of the queried locations that comprehend the spatial information of in-vivo measurements of signal characteristics transformed into a low-dimensional vector according to the vicinity of the queried points. The computed value of the descriptor is fed as the training data to learn a GP-based regressor. In particular, the RSSI metric is utilized to model the signal characteristics. The proposed approach is compared to the baseline approaches of the FSPL [25] and spatial projection (SP) based

on a GP regressor [3]. The reported results support the feasibility of the proposed approach and show significant improvements in the prediction accuracy in the extrapolation tasks.

The rest of the paper is organized as follows. A brief overview of the related work with the focus on multi-robot wireless communication is presented in Section 2. The proposed approach for communication map building is introduced in Section 3. Results of the experimental evaluation are reported and discussed in Section 4, and the work is concluded in Section 5.

2 Related work

Communication in a group of mobile robots can be understood as an instance of the *Mobile Ad-Hoc Network* (MANET). MANETs are networks with a topology that changes over time as individual network nodes change their spatial coordinates. Due to their nature, MANETs are often implemented using wireless technology allowing for more flexible communication link management. In such networks, fast and robust routing protocols [15] are needed to ensure timely packet delivery with an overhead as low as possible. Since the network nodes are dynamic, some knowledge about future signal properties need to be known in advance; a communication map can be used to obtain it.

The effect and impact of network nodes' mobility are investigated in [12], showing the importance of the prior information about nodes' behavior in multi-hop message routing problems. The current state-of-the-art multi-robot applications use prior signal or motion models to predict future positions of individual nodes and associated signal characteristics. The impact on the message routing decision-making is forthright; nodes known to leave communication range or enter signal-denied region can be disqualified from the link establishing process.

Even though communication is crucial in multi-robotic tasks, to the authors' best knowledge, the notion of the on-line building or learning a direct communication map approach is elaborated only sparsely. Most of the existing approaches use a simple fixed signal propagation model to determine whether and how well a communication link can be established between two spatial coordinates. Although a thorough review of communication modeling methods can be found in [1], a short overview of the related works is provided in the rest of this section to provide background and context of the addressed problem.

The most straightforward approach to communication modeling is the constant range method, e.g., used in [27]. It determines whether a communication link can be established between two points by comparing Euclidean distance with a threshold. Fixed-radius communication has been utilized for Kilobots [24] that use a low-power ground-directed infrared channel characterized by a relatively short and accessible communication range under the defined environmental conditions. The line-of-sight method [26] assumes that a link can be established if and only if a straight line segment connecting two spatial positions exists such that it does not intersect any obstacle. Both the fixed radius and line-of-sight methods can be combined [17].

Signal attenuation model [25] accounts for natural signal strength decay that occurs with the growing distance from the signal source. Since obstacles are not modeled, the model is called *Free-Space Path Loss* (FSPL). Its predictions of relative signal decay L_p are computed given the distance between receiver and transmitter d, their respective antennas directivities D_r, D_t, and the signal wavelength λ:

$$L_p = 10 \log_{10} \left(D_t D_r \left(\frac{\lambda}{4\pi d} \right)^2 \right). \tag{1}$$

Unlike the constant-range and line-of-sight methods, the signal attenuation model returns a continuous value of signal strength instead of the binary predictions. An extension of the attenuation modeling by considering obstacles present in the environment is presented in [14]. However, explicit knowledge about signal and material properties must be known beforehand. Thus both explorative deployments and the ability of on-line adaption to environment change are limited.

Another research path is led by Malmirchegini et al. [13], who proposed a purely probabilistic model for estimation of signal characteristics with the notion of some spatial dependence. Their model also provides mathematical reasoning about the predictability of the communication parameters. However, since their model lacks an explicit environment model, it cannot infer the attenuation thereupon; it always needs some prior measurements in the area of interest.

More sophisticated models are based on raytracing the signal propagation from the source by casting rays through the environment [22]. These models need to comprehend phenomena such as multi-path signal propagation, waveguide effect, or reflections. Hence, the raytracing-based approaches require detailed geometric environment models that include surface normals and carry information about obstacle material properties. Further, such approaches are computationally very demanding and sensitive to inaccurate or biased data about the environment that make these approaches unsuitable for on-board deployments with limited resources and field measurement devices.

The methods mentioned above tend to yield pessimistic but guaranteed results when used under particular assumptions in an austere environment. However, in sites that suffer from waveguide effect, non-trivial reflections, or non-trivial attenuation, these basic methods can return wrong predictions even in the close vicinity of the queried points. Only one group of existing approaches for communication map building is, to the best of our knowledge, based on pure machine learning without relying on any strong prior knowledge of the physical properties of the environment. In [3], a communication map is built using a spatial GP, where the core idea is to interpolate samples of communication link quality gathered in-vivo. The GP provides the most likely regression of the initially unknown signal strength function, and it interpolates the input samples together with the variance of the predicted estimates. It can thus be used to determine the most probable link quality with the confidence estimate. Consequently, the GP-based model can be utilized in active perception tasks such as [11] because information about predictive variance can be used as a valuation of the model uncertainty for the given configurations. If the whole space of all

spatial pairs is sampled with sufficiently high resolution, it is possible to predict the signal characteristics perfectly. Even though the efforts are being made to sample the whole space in [3,18], such sampling is a problem with the complexity that can be bounded by $\mathcal{O}(n^4)$ because we need to sample all (two-dimensional) coordinate pairs, which can be too costly or unfeasible. Therefore, we consider GP-based modeling to address this drawback and develop a more general model that scales better with the environment size without dense sampling before a particular deployment in the same environment.

3 Proposed Communication Map Model

The proposed approach to communication modeling follows the communication map $\mathcal{M}$ defined as a data structure with the accompanied procedure to predict a characteristic value of the communication channel for two given arbitrary positions of the transmitter and receiver placed in the environment. Thus, we formalize a generic communication map as $\mathcal{M} : \mathcal{P} \to \mathcal{R}$, where $p = \left(a_1, a_2\right) \in \mathcal{P}$ is a pair of two spatial coordinates $a = \left[a_x, a_y, a_z\right]^{\mathrm{T}} \in \mathbb{R}^3$, $r \in \mathcal{R}$ is a value characterizing the communication quality; a_1 is the position of the transmitter, a_2 of the receiver. We assume w.l.o.g. r is a scalar $\mathcal{R} \subseteq \mathbb{R}$ for the sake of simplicity in this paper; in particular, r is a value of the RSSI.

The mapping $\mathcal{M}$ is realized by a descriptor function δ chained to the GP regressor[21] $\mathcal{G}|_X$. Formally, $\mathcal{M} = \delta \circ \mathcal{G}|_X$, where X is a set of the training data. Since the GP output provides the predictions associated with predictive variance, the GP-based regression is suited for active perception scenarios, where the learner improves its model by adding new samples for configurations with high predictive variance. Hence, we follow the GP-based approach [3]. However, the key novelty is in the proposed descriptor function that provides data such as distance between the queried locations or obstacle occupancy metric. Thus, unlike the approach [3], the proposed method provides low-variance predictions also in spatially unexplored locations given the corresponding descriptor value is correlated to some previously sampled measurement's descriptor.

3.1 Gaussian Process

We use GP regressors in each model to infer the signal strength from samples transformed by respective descriptors. In this section, we briefly describe the GP regression to make the paper self-contained. First, let the function of interest $f(x)$ be observed with Gaussian noise ϵ

$$y = f(x) + \epsilon, \quad \epsilon \in \mathcal{N}(0, \sigma^2). \tag{2}$$

The GP is then a distribution over all possible functions [21]

$$f(x) \sim \mathcal{GP}(m(x), K(x, x')), \tag{3}$$

where $m(x)$ and $K(x, x')$ are the mean and covariance, respectively, defined as

$$m(x) = E\left[f(x)\right], \tag{4}$$
$$K(x, x') = E\left[\left(f(x) - m(x)\right)\left(f(x') - m(x')\right)\right]. \tag{5}$$

The latent values f_* of testing data X_* are computed given training data X as

$$\begin{aligned} \mu(X_*) &= K(X, X_*)\left[K(X, X) + \sigma^2 I\right]^{-1} y, \\ (\sigma(X_*))^2 &= K(X_*, X_*) \\ &\quad - K(X, X_*)^T\left[K(X, X) + \sigma^2 I\right]^{-1} K(X, X_*), \end{aligned} \tag{6}$$

where $K(X, X')$ is the covariance function. Two distinct covariance functions were used in individual descriptors; the first is the squared exponential kernel

$$K(x, x') = \sigma^2 \exp\left(-\frac{\|x - x'\|_2}{2l^2}\right), \tag{7}$$

where σ^2 is the output variance and l is the lenghtscale. The second covariance function is the Matern $3/2$ kernel

$$K(x, x') = \sigma^2 \frac{2^{1-3/2}}{\Gamma(3/2)}\left(\sqrt{3}\frac{\|x - x'\|_2}{l}\right)^{3/2} L_{3/2}\left(\sqrt{3}\frac{\|x - x'\|_2}{l}\right), \tag{8}$$

with σ and l defined analogously as before, Γ being the gamma function and $L_{3/2}$ the modified Bessel function of the second kind.

3.2 Descriptor Functions in GP-based Communication Map

The GP can be coupled with a descriptor function characterizing the input data; three different functions are considered. The first descriptor (9) is the spatial projection utilized in [3] further denoted also as $\delta_{\text{spatial}}(p)$, where the descriptor is a four-dimensional vector created by truncating the z-axis coordinates of the pose vectors a_a, a_b

$$\delta_{\text{spatial}}(p) = \delta_{\text{spatial}}\left(\left(\begin{bmatrix} a_{1x} \\ a_{1y} \\ a_{1z} \end{bmatrix}, \begin{bmatrix} a_{2x} \\ a_{2y} \\ a_{2z} \end{bmatrix}\right)\right) = \begin{bmatrix} a_{1x} \\ a_{1y} \\ a_{2x} \\ a_{2y} \end{bmatrix}. \tag{9}$$

The second examined descriptor δ_{FSPL} is based on Euclidean distance between the two pose vectors in p. It follows the FSPL [25] signal attenuation model under the assumption that both the signal transmitter and receiver are omnidirectional and the environment is without obstacles. However, when it is combined with the GP regressor, it provides the estimate of the mean signal strength and its variance. The descriptor is defined as

$$\delta_{\text{FSPL}}\left(p\right) = \left[\|p\|_2\right], \tag{10}$$

where $\|p\|_2$ is the three-dimensional Euclidean distance

$$\|p\|_2 = \left\| \left(\begin{bmatrix} a_{1x} \\ a_{1y} \\ a_{1z} \end{bmatrix}, \begin{bmatrix} a_{2x} \\ a_{2y} \\ a_{2z} \end{bmatrix} \right) \right\|_2 = \left\| \begin{bmatrix} a_{1x} - a_{2x} \\ a_{1y} - a_{2y} \\ a_{1z} - a_{2z} \end{bmatrix} \right\|_2 . \tag{11}$$

Finally, the third proposed descriptor is called the *Projected Free Space Ratio* (PFSR) denoted δ_{PFSR}. It extends the FSPL-based descriptor by examining obstacles between the connection of two locations using the available map of the environment. The descriptor δ_{PFSR} is a two-dimensional vector, where the first dimension corresponds to δ_{FSPL}. The second dimension is defined as the ratio of the occupied and free space along the straight line connecting the queried points a_1 and a_2. However, since the exact volumetric computation is not practical due to data noise, we use a robust off-line estimation of the environment.

The environment map is based on point cloud built from depth measurements of RGB-D or LiDAR sensors localized to the same reference frame as the pose vectors a. For model learning and inference, the point cloud is discretized into an equally-sized spatial grid summed along the vertical axis. The resulting two-dimensional grid is normalized by the maximum value and thresholded to create a binary occupancy grid. After that, Canny edge detector [9] with eight-fold image erosion and dilation gap-filling technique is performed. Then, given two query points, a_1 and a_2, a set of grid cells intersected by the straight-line $\mathcal{B}(p)$ between the points' ground plane projections is generated using Bresenham's line algorithm [8].

The proposed PFSR descriptor δ_{PFSR} is defined as

$$\delta_{\mathrm{PFSR}}(p) = \begin{bmatrix} \|p\|_2 \\ O(p) \end{bmatrix}, \tag{12}$$

with the occupied ratio $O(p)$ computed as

$$O(p) = \frac{\sum_{b \in \mathcal{B}(p)} occupied(b)}{|\mathcal{B}(p)|}, \tag{13}$$

where $occupied(b)$ returns 1 if the cell b is occupied and 0 otherwise.

4 Results

The prediction of the signal strength using all three introduced descriptors employed in GP-based regression has been examined with real experimental data. We also compare the GP-based models with pure FSPL model [25] as defined in (1). All the methods have been implemented in C++ using Limbo [10]. The GP-based regressor with the descriptor $\delta_{\mathrm{spatial}}(p)$ has been used with the exponential kernel (7) as in [3]. The same kernel is also utilized with $\delta_{\mathrm{FSPL}}(p)$ because of the identical dimension as for $\delta_{\mathrm{spatial}}(p)$. However, Matern three-halves function (8) has been used with $\delta_{\mathrm{PFSR}}(p)$ because better results have been achieved

Table 1. Utilized hyperparameters in GP-based communication models.

Descriptor	$\delta_{\text{spatial}}(p)$ [3]	$\delta_{\text{FSPL}}(p)$	$\delta_{\text{PFSR}}(p)$
Kernel function	Exponential (7)	Exponential (7)	Matern $^3/_2$ (8)
Prior constant mean	-45.00	-45.00	-45.00
l	1.17	0.50	10.00
σ	0.01	0.37	0.05

than with the exponential kernel. We used a grid-search method to find the individual hyperparameters; the best performing values in the cross-validation are listed in Table 1.

The training and testing dataset has been collected using measured RSSI in the *Bull Rock* cave system using communication nodes with RFM69HCW transceiver [23] with an output power of 100 mW operating at 868 MHz that exhibits better around-corner propagation in comparison, e.g., to 2.5 GHz and 5.0 GHz [28]. The module uses a quarter wavelength long whip antenna and frequency-shift keyring (FSK) modulation schema. Direct measurement of the RSSI is provided via the internal module circuitry. The RSSI value is numerically equal to the measured received signal power in units of dBm, rounded to the nearest integer. The RSSI measurements are accompanied by spatial information from the Leica TS16 total station. The used environment map for the descriptor $\delta_{\text{PFSR}}(p)$ has been built using a point cloud assembled from eight full-dome scans captured by Leica BLK360; each scan contained roughly five million points.

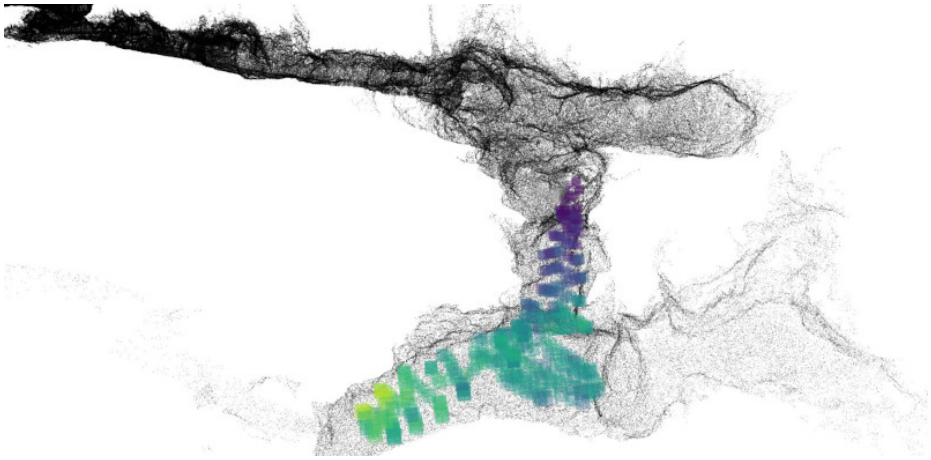

Fig. 1. Visualization of the created environment model of the testing area in the *Bull Rock* cave system. The localized point cloud is shown in black color, and a part of the localized RSSI measurements is depicted in the yellow-purple color map. The yellow color represents full received signal strength; purple samples are those with a more attenuated signal. The figure presents a situation with the transmitter position near the cave entrance.

The whole dataset contains about 4500 samples of the RSSI with the positions of both transmitter and receiver registered to the global reference frame. The samples have been collected by fixing the transmitter at five different locations and moving the receiver through the testing area. A visualization of the created model of the environment is depicted in Fig. 1. An example of the created grid map utilized for computing *occupied*(b) in (13) is shown in Fig. 2. The communication models are evaluated in two setups assessing interpolation and extrapolation capabilities, respectively.

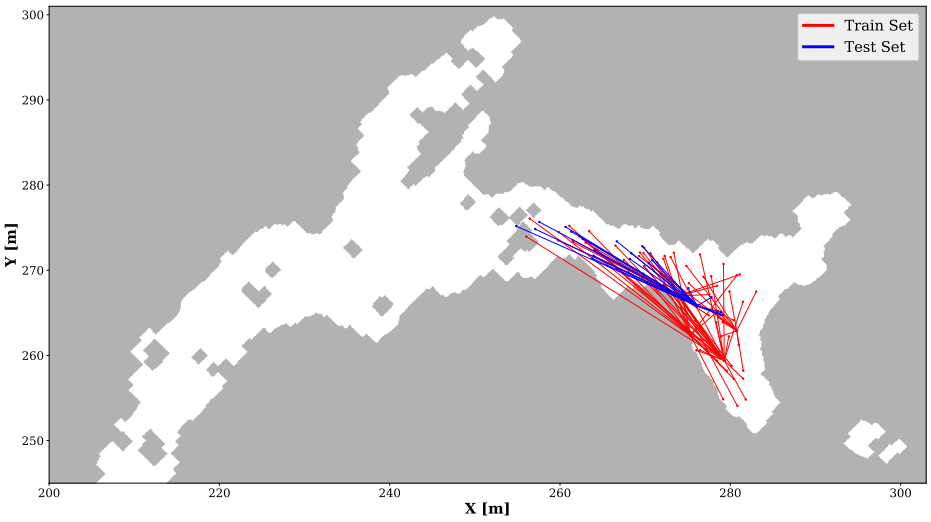

Fig. 2. A cutout of the relevant area of the occupancy grid with an instance of dataset in extrapolation setup. Training part is depicted in the red and testing dataset in the blue.

Table 2. Cross-validation results of RSSI prediction in the interpolation setup.

Method	FSPL [25]	$\delta_{\text{spatial}}(p)$ [3]	$\delta_{\text{FSPL}}(p)$	$\delta_{\text{PFSR}}(p)$
MAE [dBm]	8.99	4.05	8.19	6.51
RMSE [dBm]	11.31	5.46	10.01	8.93

Monte Carlo cross-validation schema has been used for evaluation in the interpolation setup. The dataset has been randomly divided into a training set and testing set 10 times with the train-to-test set size ratio $1 : 9$, producing mutually independent data. The results of the interpolation cross-validation are summarized in Table 2, where MAE stands for the *Mean Absolute Error* and RMSE for the *Root Mean Squared Error*.

Table 3. Cross-validation results of RSSI prediction in the extrapolation setup.

Method	FSPL [25]	$\delta_{\text{spatial}}(p)$ [3]	$\delta_{\text{FSPL}}(p)$	$\delta_{\text{PFSR}}(p)$
MAE [dBm]	9.08	16.62	7.71	7.88
RMSE [dBm]	11.42	21.30	9.77	10.37

For the evaluation of the methods in the extrapolation setup, one representative transmitter location with associated measurements has been utilized as the test set; the rest of the dataset has been utilized as the training set. The evaluation results are reported in Table 3. Although the reported results are not statistically significant due to the size of the dataset, the proposed method with $\delta_{\text{PFSR}}(p)$ can learn with similar results to $\delta_{\text{FSPL}}(p)$, still beating the FSPL [25]. It is particularly important because the results support the fact that the proposed method can overcome an inherent drawback of the spatial GP [3] in its inability to spatially extrapolate as indicated for $\delta_{\text{spatial}}(p)$ in Table 3, where the results are even worse than the simple FSPL model.

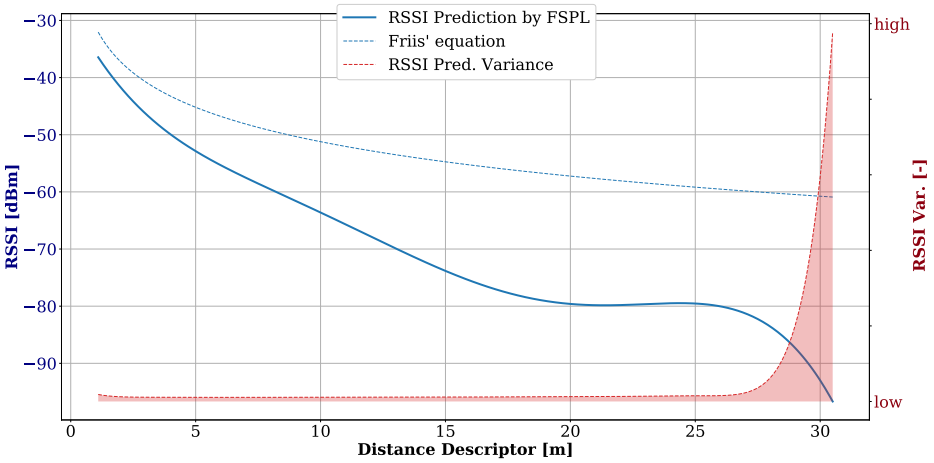

Fig. 3. RSSI predicted while utilizing $\delta_{\text{FSPL}}(p)$ as a function of the distance only and its prediction variance. The FSPL model assumes omnidirectional antennas, and it is parametrized with the nominal frequency 868 MHz.

In addition to the cross-validation, we further investigate the examined descriptor functions. The descriptor space of $\delta_{\text{FSPL}}(p)$ can be understood as regression of the FSPL [25] applied in an obstructed environment. The prediction plot is shown in Fig. 3. Analogously, the descriptor space of $\delta_{\text{PFSR}}(p)$ is depicted in Fig. 4. Expectedly, the values predicted by the GP are greatly outlying in areas where sparse or no samples have been taken as it can be seen in the top right part of the plot.

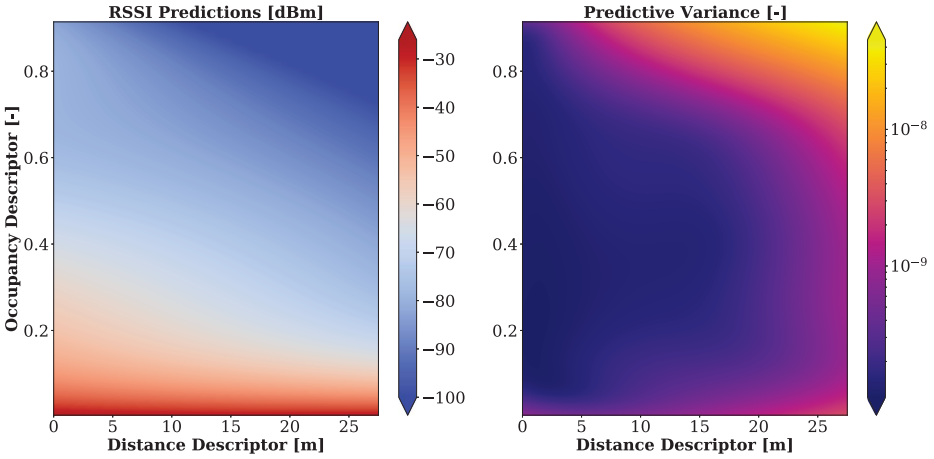

Fig. 4. Predicted RSSI mean values with variances in the descriptor space of $\delta_{\mathrm{PFSR}}(p)$. The plots are clipped to the interval $[-20, -100]$ dBm because the underlying GP predicts highly outlying values in unobserved feature-value regions with high variances.

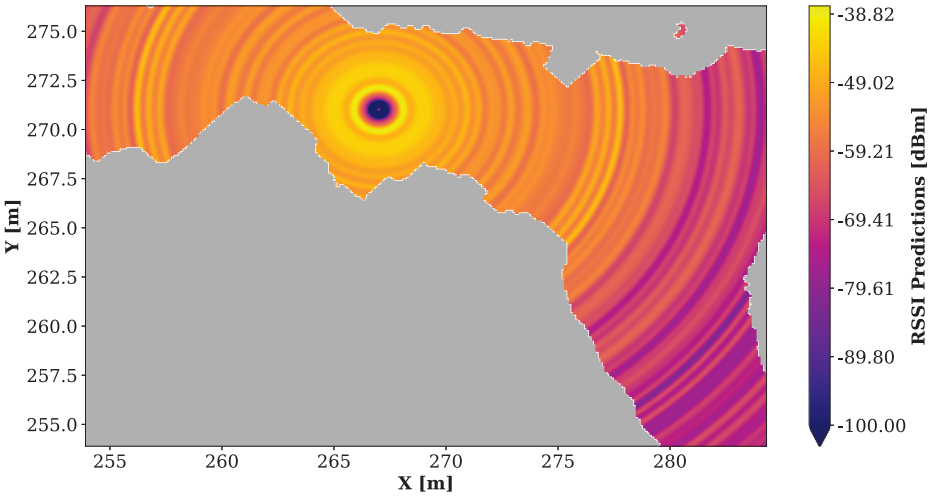

Fig. 5. Illustration of extrapolated communication map for fixed transmitter $\delta_{\mathrm{FSPL}}(p)$.

Finally, we provide examples of the extrapolated predictions for the $\delta_{\mathrm{FSPL}}(p)$ and $\delta_{\mathrm{PFSR}}(p)$ descriptors in Fig. 5 and Fig. 6, respectively. The figures illustrates that the proposed descriptor $\delta_{\mathrm{PFSR}}(p)$ is able to account for obstacles whereas $\delta_{\mathrm{FSPL}}(p)$ accounts only for the distance.

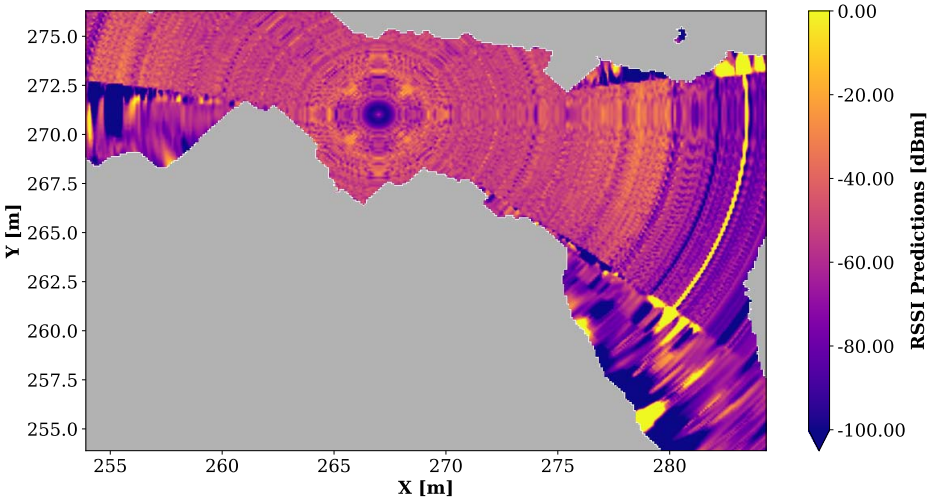

Fig. 6. Illustration of extrapolated communication map for fixed transmitter $\delta_{\mathrm{PFSR}}(p)$.

5 Conclusion

In this paper, we report on building communication maps using a GP-based framework with three different descriptor functions. We propose a novel descriptor function that characterizes the area between the signal source and receiver. The proposed approach extrapolates the RSSI values with accuracy an order of magnitude better than the state-of-the-art method based on the spatial GP regressor. For future work, we aim to improve the prediction by designing more informative descriptor functions. Besides, we also aim to collect a larger representative dataset by exploiting novel self-localizing handheld device [5].

Acknowledgment

The presented work has been supported under the OP VVV funded project CZ.02.1.01/0.0/0.0/16_019/0000765 "Research Center for Informatics" and the Czech Science Foundation (GAČR) under research Projects 18-18858S and GA20-29531S. We like to acknowledge the support of the speleologist branch organization ZO 6-01 for providing access to the Bull Rock cave testing site.

References

1. Amigoni, F., Banfi, J., Basilico, N.: Multirobot exploration of communication-restricted environments: A survey. IEEE Intelligent Systems **32**(6), 48–57 (2017). DOI: 10.1109/MIS.2017.4531226

2. Amigoni, F., Banfi, J., Basilico, N., Rekleitis, I., Quattrini Li, A.: Online update of communication maps for exploring multirobot systems under connectivity constraints. In: Distributed Autonomous Robotic Systems. pp. 513–526 (2019). DOI: 10.1007/978-3-030-05816-6_36
3. Banfi, J., Li, A.Q., Basilico, N., Rekleitis, I., Amigoni, F.: Multirobot online construction of communication maps. In: IEEE International Conference on Robotics and Automation (ICRA). pp. 2577–2583 (2017). DOI: 10.1109/ICRA.2017.7989300
4. Banfi, J.: Recent advances in multirobot exploration of communication-restricted environments. Intelligenza Artificiale **13**(2), 203–230 (2019). DOI: 10.3233/IA-180013
5. Bayer, J., Faigl, J.: Handheld localization device for indoor environments. In: International Conference on Automation, Control and Robots (ICACR). pp. 60–64 (2020). DOI: 10.1109/ICACR51161.2020.9265494
6. Berglund, E., Sitte, J., Wyeth, G.: Active audition using the parameter-less self-organising map. Autonomous Robots **24**(4), 401–417 (May 2008). DOI: 10.1007/s10514-008-9084-9
7. Bildea, A., Alphand, O., Rousseau, F., Duda, A.: Link quality estimation with the gilbert-elliot model for wireless sensor networks. In: IEEE Annual International Symposium on Personal, Indoor, and Mobile Radio Communications (PIMRC). pp. 2049–2054 (2015). DOI: 10.1109/PIMRC.2015.7343635
8. Bresenham, J.E.: Algorithm for computer control of a digital plotter. IBM Systems Journal **4**(1), 25–30 (1965). DOI: 10.1147/sj.41.0025
9. Canny, J.: A computational approach to edge detection. IEEE Transactions on Pattern Analysis and Machine Intelligence **PAMI-8**(6), 679–698 (1986). DOI: 10.1109/TPAMI.1986.4767851
10. Cully, A., Chatzilygeroudis, K., Allocati, F., Mouret, J.B.: Limbo: A Flexible High-performance Library for Gaussian Processes modeling and Data-Efficient Optimization. The Journal of Open Source Software **3**(26), 545 (2018). DOI: 10.21105/joss.00545
11. Luo, W., Sycara, K.: Adaptive Sampling and Online Learning in Multi-Robot Sensor Coverage with Mixture of Gaussian Processes. In: IEEE International Conference on Robotics and Automation (ICRA). pp. 6359–6364 (2018). DOI: 10.1109/ICRA.2018.8460473
12. Maan, F., Mazhar, N.: MANET routing protocols vs mobility models: A performance evaluation. In: International Conference on Ubiquitous and Future Networks (ICUFN). pp. 179–184 (2011). DOI: 10.1109/ICUFN.2011.5949158
13. Malmirchegini, M., Mostofi, Y.: On the spatial predictability of communication channels. IEEE Transactions on Wireless Communications **11**(3), 964–978 (2012). DOI: 10.1109/TWC.2012.012712.101835
14. Micheli, D., Delfini, A., Santoni, F., Volpini, F., Marchetti, M.: Measurement of electromagnetic field attenuation by building walls in the mobile phone and satellite navigation frequency bands. IEEE Antennas and Wireless Propagation Letters **14**, 698–702 (2015). DOI: 10.1109/LAWP.2014.2376811
15. Mohseni, S., Hassan, R., Patel, A., Razali, R.: Comparative review study of reactive and proactive routing protocols in MANETs. In: IEEE International Conference on Digital Ecosystems and Technologies. pp. 304–309 (2010). DOI: 10.1109/DEST.2010.5610631
16. Muralidharan, A., Mostofi, Y.: Statistics of the distance traveled until successful connectivity for unmanned vehicles. Autonomous Robots **44**(1), 25–42 (2020). DOI: 10.1007/s10514-019-09850-7

17. Nestmeyer, T., Robuffo Giordano, P., Bülthoff, H.H., Franchi, A.: Decentralized simultaneous multi-target exploration using a connected network of multiple robots. Autonomous Robots **41**(4), 989–1011 (2017). DOI: 10.1007/s10514-016-9578-9
18. Penumarthi, P.K., Li, A.Q., Banfi, J., Basilico, N., Amigoni, F., O'Kane, J., Rekleitis, I., Nelakuditi, S.: Multirobot exploration for building communication maps with prior from communication models. In: International Symposium on Multi-Robot and Multi-Agent Systems (MRS). pp. 90–96 (2017). DOI: 10.1109/MRS.2017.8250936
19. Qin, J., Wei, Z., Qiu, C., Feng, Z.: Edge-prior placement algorithm for uav-mounted base stations. In: IEEE Wireless Communications and Networking Conference (WCNC). pp. 1–6 (April 2019). DOI: 10.1109/WCNC.2019.8885992
20. Quattrini Li, A., Penumarthi, P.K., Banfi, J., Basilico, N., O'Kane, J.M., Rekleitis, I., Nelakuditi, S., Amigoni, F.: Multi-robot online sensing strategies for the construction of communication maps. Autonomous Robots **44**(3), 299–319 (2020). DOI: 10.1007/s10514-019-09862-3
21. Rasmussen, C.E., Williams, C.K.I.: Gaussian processes for machine learning. Adaptive computation and machine learning, MIT Press, Cambridge, Mass (2006), http://www.gaussianprocess.org/gpml
22. Remley, K.A., Anderson, H.R., Weisshar, A.: Improving the accuracy of ray-tracing techniques for indoor propagation modeling. IEEE Transactions on Vehicular Technology **49**(6), 2350–2358 (2000). DOI: 10.1109/25.901903
23. Rouček, T., Pecka, M., Čížek, P., Bayer, J., Šalanský, V., Heřt, D., Petrlík, M., Báča, T., Spurný, V., Pomerleau, F., Kubelka, V., Faigl, J., Zimmermann, K., Saska, M., Svoboda, T., Krajník, T.: Darpa subterranean challenge: Multi-robotic exploration of underground environments. In: 2019 Modelling and Simulation for Autonomous Systems (MESAS). pp. 274–290 (2020). DOI: 10.1007/978-3-030-43890-6_22
24. Rubenstein, M., Ahler, C., Hoff, N., Cabrera, A., Nagpal, R.: Kilobot: A low cost robot with scalable operations designed for collective behaviors. Robotics and Autonomous Systems **62**(7), 966–975 (2014). DOI: 10.1016/j.robot.2013.08.006
25. Shaw, J.A.: Radiometry and the Friis transmission equation. American Journal of Physics **81**(1), 33–37 (2013). DOI: 10.1119/1.4755780
26. Stump, E., Michael, N., Kumar, V., Isler, V.: Visibility-based deployment of robot formations for communication maintenance. In: IEEE International Conference on Robotics and Automation (ICRA). pp. 4498–4505 (2011). DOI: 10.1109/ICRA.2011.5980179
27. Weihua Sheng, Qingyan Yang, Song Ci, Ning Xi: Multi-robot area exploration with limited-range communications. In: IEEE/RSJ International Conference on Intelligent Robots and Systems (IROS). vol. 2, pp. 1414–1419 (2004). DOI: 10.1109/IROS.2004.1389594
28. Zhou, C., Plass, T., Jacksha, R., Waynert, J.A.: Rf propagation in mines and tunnels: Extensive measurements for vertically, horizontally, and cross-polarized signals in mines and tunnels. IEEE Antennas and Propagation Magazine **57**(4), 88–102 (2015). DOI: 10.1109/MAP.2015.2453881